A PREMILINARY STUDY OF THE OECD/NEA 3D TRANSPORT PROBLEM USING THE LATTICE CODE DRAGON

N. Martin, G. Marleau, A. Hébert
Institut de génie nucléaire, École Polytechnique de Montréal
C.P. 6079, succ. Centre-ville, Montréal, Québec, CANADA H3C 3A7

Abstract

In this paper we present a premilinary analysis of the NEA3D-TAB-2007 transport problem proposed by the OECD/NEA expert group on radiative transfer. This computational benchmark was originally proposed by Y. Azmy in 2007 to test the performance of 3D transport methods and codes over a suite of problems defined by large variations in space parameters. Two deterministic methods were applied to generate the numerical solutions: the discrete ordinates method (S_N), and the method of open characteristics of I.R. Suslov (MCCG). We provide comparisons between MCNP reference solutions and MCCG and DRAGON-S_N results in order to reveal the advantages and limitations of both methods.

I. Introduction

The lattice code DRAGON [1] can solve 3D transport problems using various numerical methods. Collision probabilities (CP) were implemented first and are still widely used for lattice transport calculations. More recently, an open characteristics flux solution has been made avalaible in 2D/3D [2] and discrete ordinates method have been extended to regular 3D Cartesian geometries [3]. We propose in this paper to apply both methods to the NEA3D-TAB-2007 benchmark [4], and then to compare the numerical results generated by DRAGON with MCNP reference solutions.

II. Presentation of the problem

The geometry defining the benchmark consists in two embedded parallelepipeds, as depicted in Figure 1. The outer is referred to with the index 1 and has a unit square base and height L, while the inner is referenced with the index 2 and is scaled down by a parameter γ, i.e., it has dimensions $\gamma \times \gamma \times \gamma L$. Vacuum boundary conditions are imposed on all the external faces. A fixed, distributed unit source with dimension $(1-\gamma)/2, (1-\gamma)/2, L \times (1-\gamma)/2$ is localised at the origin as shown in Figure 2. The total macroscopic section and the scattering ratio are denoted as Σ_i and c_i respectively, with i=1 or 2. The suite of benchmarks is then defined by varying all the

parameters L, γ, Σ_1, c_1, Σ_2, c_2, with the range of variation provided in Table 1. As each quantity can take three values, we obtain a total number of 3^6=729 cases.

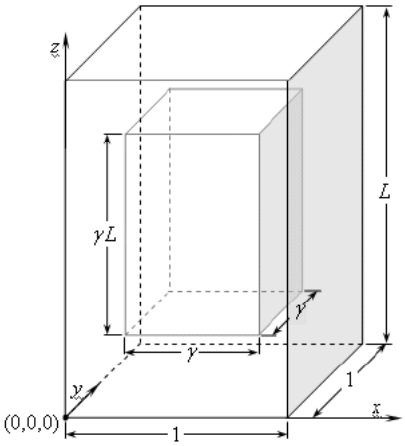

Figure 1: Geometric configuration of the benchmark

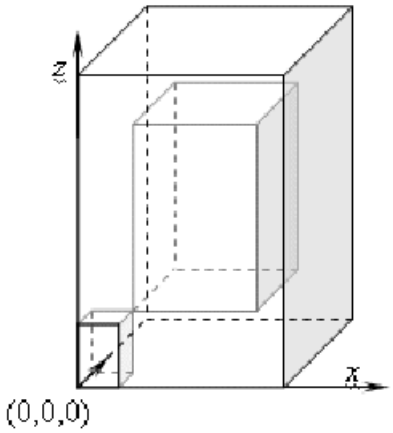

Figure 2: Localisation of the source

Table 1: Range of parameters

Parameters	Values		
L	0.1	1.0	5.0
γ	0.1	0.5	0.9
Σ_1	0.1	1.0	5.0
c_1	0.5	0.8	1.0
Σ_2	0.1	1.0	5.0
c_2	0.5	0.8	1.0

III. Computational strategy

In this section, we describe the options used for generating numerical solutions to the benchmark. Three main parameters are to be set for both methods, i.e., spatial order of integration, angular quadrature order, and the inner iteration acceleration strategy selected for each solution algorithm.

III.A. S_N computational strategy

Let us first consider the spatial integration strategy. The discrete ordinates method available in the lattice code DRAGON is based on a generalization of the classical diamond differencing (DD) scheme. Linear Diamond differencing (LD) scheme, which is equivalent to classical DD scheme, is the option by default. We have used parabolic DD scheme, so as to introduce high-order S_N results. A cubic order solution was also programmed, but it introduces numerical instabilities in some cases. For the angular quadrature, we have used a level-symmetric quadrature (LQ_n), restricted to S_{20} order. A Legendre-Chebychev angular quadrature is also available up to order S_{64}, but due to memory limitations, we were not able to provide a complete suite of solutions for the benchmark when $n > 32$. In addition, it was shown that for this benchmark, a P_n-T_n quadrature with n=32 is less accurate that LQ_n quadrature with n=20. Acceleration strategy of the source iterations is an important issue for the S_N method. In case of strong heterogenous and highly diffusive medias, inner iterations may converge very slowly[8]. Hence, we use a Diffusion Synthetic Acceleration (DSA)[9] preconditionning of the S_N method conjugated with a Krylov subspace method, GMRES(m)[10]. This strategy has been proven very effective for all the cases of the benchmark.

Options used in the S_N solver are:

- Parabolic Diamond-Differencing scheme.
- Uniform spatial discretization of the regular geometry by $subm$.
- S_n Level-symmetric quadrature (LQ_n), $n \leq 20$.

- DSA-preconditionning and GMRES(10) acceleration of the inner iterations.
- 10^{-5} convergence criterion.

Two parameters will vary namely $subm$, the level of spatial discretization, and n, the order of the angular quadrature.

IV. MOC computational strategy

The set of options for this solver are more numerous than for the S_N case and include parameters in both geometry tracking module and MOC flux solver itself.[2] Premilinary studies have shown that a high track density is mandatory, due to small dimensions of computational cells required to insure low relative error. Furthermore, an attempt was made to use a 3D prismatic MOC formalism, however strong restrictions appeared, due to numerical instabilities of the traking operator. This occured when relative errors generated by the 3D prismatic extension of the tracking module NXT: are very close to machine numerical precision. As a consequence, we were compelled to use the full 3D traking operator, in such a way that CPU time for generating the tracking lines combined with the flux resolution made the MOC solution was far more expensive in computing ressources than the S_N method. Regarding the source integration, a step characteristics (SC) and a diamond differencing (DD) strategy are avalaible. We used for this benchmark the DD scheme, which is slightly better than the SC for a given spatial discretization. For the angular discretization, a Legendre-Chebychev (P_n-T_n) quadrature was selected. Concerning the source integration strategy, in order to reduce computational ressources, no asymptotical treatment of the vanishing sources is applied and tabulated exponentials are used. To insure faster convergence of the inner iterations, a SCR-preconditionning (Self-Collision Rebalancing) [6] is combined with an Krylov subspace method, GMRES(m). The ACA-preconditionning (algebraic collapsing acceleration)[5] has been established as a more powerfull procedure to reduce inner iterations, however in monokinetic problems, ACA leads to a large overhead in term of computational ressource. As a result, SCR is faster than ACA in terms of CPU time.

Options used are in the tracking module NXT:

- Uniform discretization of the geometry by a factor of $subm$.
- Track density ρ (density of integration lines in cm^{-2}).
- Angular quadrature of type P_n-T_n with $nangl$, value lower than 46.

MCCG flux solver options are:

- Diamond Differencing scheme along the tracking lines.
- No asymptotical treatment for vanishing optical thicknesses.
- SCR preconditionning of inner iterations.

- GMRES(m) Krylov Subspace method for accelerating SCR preconditionned inner iteration.
- 10^{-5} convergence criterion.

Hence, for the MCCG solutions, the parameters that will be changed to generate the three required runs are:

1. $subm$, corresponding to the level of mesh refinement of the geometry.
2. ρ, the track density.
3. $nangl$, the angular quadrature order.

V. MCNP computational strategy

We present briefly the strategy adopted by the organizers to provide MCNP5 solutions for the entire suite of benchmarks. Since this study is done using temporary MCNP5 reference solutions, note that for some cases, Monte-Carlo solutions exhibit 0 scoring or significant statistical error. All Monte-Carlo results used in this work are obtained with 2 billion particle histories. Final reference MCNP5 solutions are expected to be computed using a suitable biasing method, such as a variance reduction technique [7].

VI. Parametric study

In this section, we briefly present the parametric study performed with both the MOC and S_N numerical methods. The procedure applied here is quite simple albeit fastiduous, and is usually reffered as model refinement. It consits in increasing the order of angular and spatial discretization, to observe a linear decrease in error. We finally obtain minimas for our level of angular and spatial discretizations for which our numerical solutions are in the asymptotic regime. In some cases, increasing the level of discretization may lead to an increase in error: this is mainly due to shortcomings of the method invoked during the generation of the numerical solutions. The methodology applied for both methods involved an independent study of the angular and spatial quadrature parameters. Hence, we initially impose a relatively fine spatial discretization, and increase progressively the order of the angular quadrature. Once the angular quadrature has converged, the spatial quadrature is coarsened progressively (decrease in the order of the spatial quadrature). Note that for MCCG calculations, the density of tracking is another variable of great influence. We then assume that the combined minimums in space and angle discretizations is sufficient to ensure that the asymptotic regime has been reached. This is not a rigorous method, especially when a strong coupling exists between space and angular variables, as it occurs when streaming effects are important. To avoid this issue, we have selected the case 222222, defined by $L = 1.0$; $\gamma = 0.5$; $\Sigma_1 = \Sigma_2 = 1.0$ and $c_1 = c_2 = 0.8$.

For the spatial mesh studies, a S_{20} quadrature order is imposed respectively for the S_N method, and $nangl$=32 for the MCCG solver. In Figures 3 and 4, the L_2 norm is a scalar quantity whose value represents the size (or length) of a vector error corresponding to a given discretization:

$$err = \sqrt{\sum_{i=1}^{15} \left(\Phi^i_{\text{computed}} - \Phi^i_{\text{MCNP}}\right)^2}$$

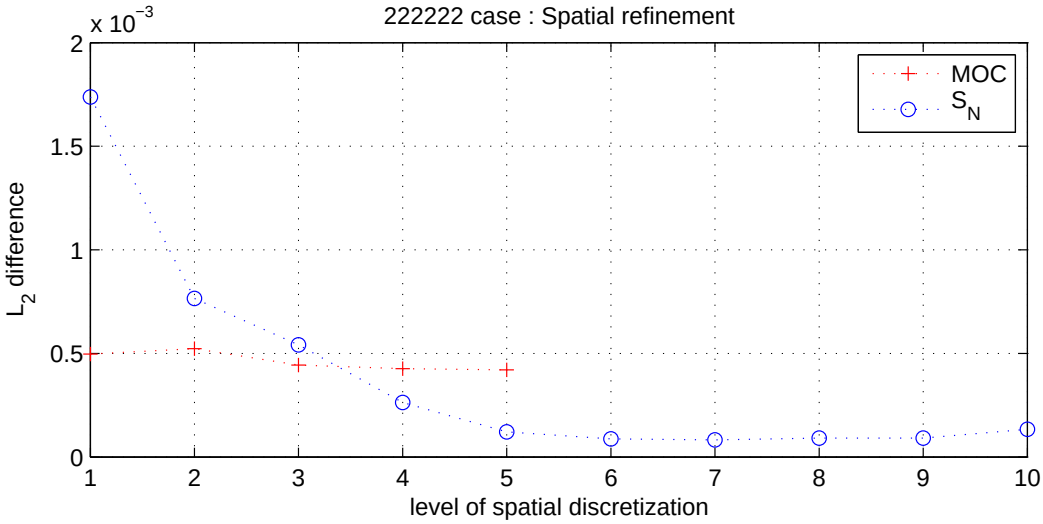

Figure 3: Mesh refinement

For the angular study, we impose respectively $subm$=4 and $subm$=8 respectively for the S_N and MCCG methods. The difference between our results and those of MCNP are then presented in Figure 4.

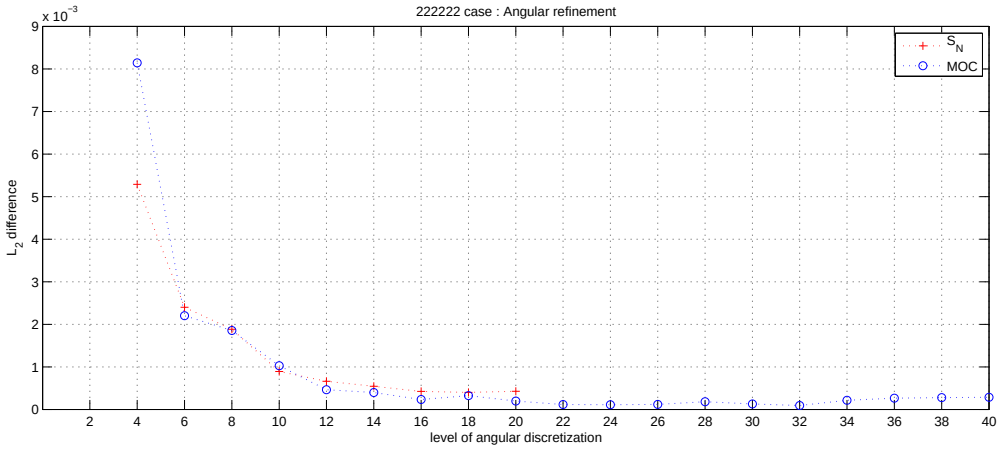

Figure 4: Mesh refinement

We clearly observe that our MOC numerical solutions are not in the asymptotic regime when angular and spatial discretization are set to their maximums. Error oscillations occur, both for angular and spatial parameters. Nethertheless, we could assume that for a spatial discretization in the range between 4 and 8, and an angular disretization greater than 20, the relative errors are acceptable. S_N numerical results approach MCNP solutions for a spatial discretization greater than 2, and when angular quadrature is greater than S_{16}.

VI.A. Generation of the results

The parametric study exposed before allows us to select three level of discretization, both for angular and spatial parameters, in order to generate for our two numerical method the set of results required for the whole suite of the benchmarks.

Accordingly, for the S_N case we selected:

1. A uniform spatial discretization of the regular geometry by $subm$=2 with a S_{16} level-symmetric quadrature.
2. A uniform spatial discretization of the regular geometry by $subm$=3 with a S_{18} level-symmetric quadrature.
3. A uniform spatial discretization of the regular geometry by $subm$=4 with a S_{20} level-symmetric quadrature.

For the MOC solutions, the MCCG flux solver options remain the same and only the parameters associed with the tracking module are modified:

1. An uniform discretization of the geometry by a factor of 2 with track density of 5×10^2 integration lines in cm^{-2}. and an angular quadrature of type P_n-T_n with $nangl$=16.

2. An uniform discretization of the geometry by a factor of 3 with a track density of 5×10^2 integration lines in cm^{-2} and an angular quadrature of type P_n-T_n with $nangl$=24.

3. An uniform discretization of the geometry by a factor of 4 with a track density of 1×10^3 integration lines in cm^{-2} and an angular quadrature of type P_n-T_n with $nangl$=32.

VII. Analysis of the results

In this section, we provide comparison of our S_N and MCCG numerical results with the MCNP reference solutions. The large number of data generated, typically 15×729 per run, burdens strongly the analysis. We choose to use the mean relative error by case, namely:

$$\delta_n(\%) = \frac{1}{15} \sum_{i=1}^{15} \frac{\Phi^i_{\text{computed}} - \Phi^i_{\text{MCNP}}}{\Phi^i_{\text{MCNP}}}$$

Hence, we will establish the total number of cases n that satisfy a criterion on the mean relative error:

$$\delta_n \leq \epsilon$$

with ϵ a tolerance on the mean relative error in %.

Another option is to compute the number n of cases between two bounding error limits as:

$$\epsilon_1 \leq \delta_n \leq \epsilon_2$$

with ϵ_1 and ϵ_2 tolerances on the mean relative error in %. We can then define the number n as a function of ϵ, which leads to a straightforward evaluation of the performance of a method. The distribution of results and the cumulative distribution as a function of error are presented respectively in Figures 5 and 6.

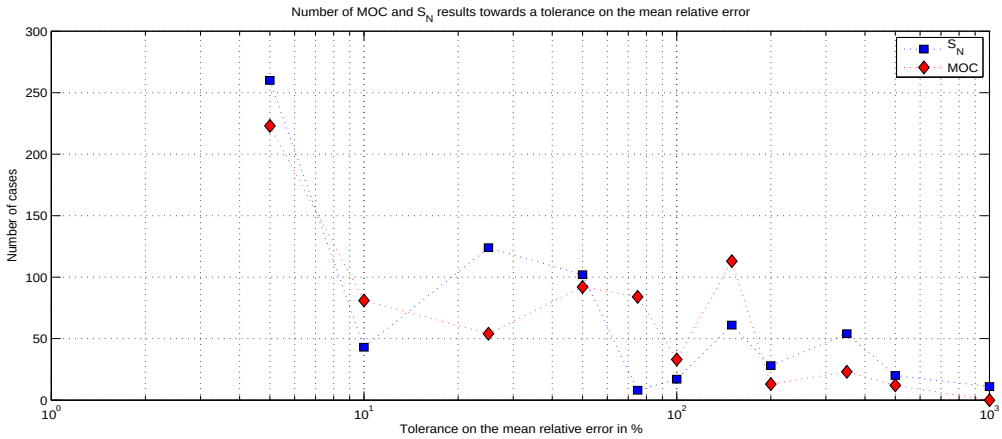

Figure 5: Distribution of results in function of the mean relative error

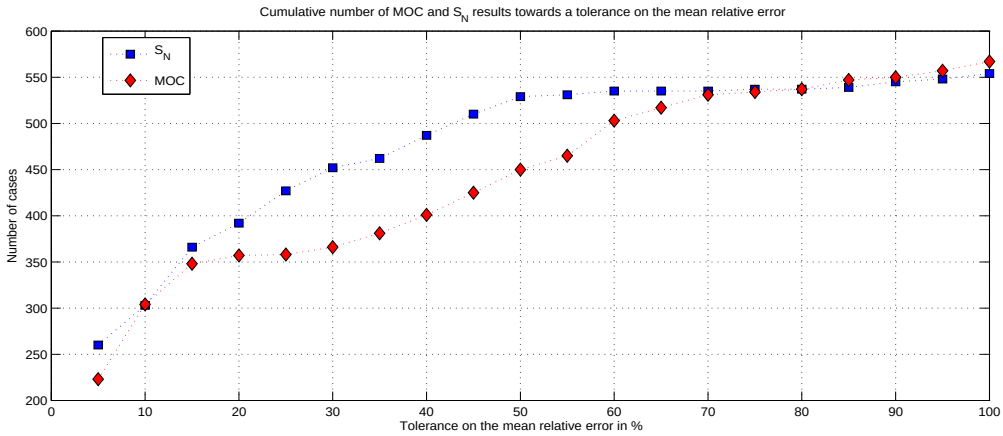

Figure 6: Cumulative distribution of results in function of the mean relative error

At the light of theses figures, we notice that the computational challenge raised by this benchmark is a source of large relative errors between for both MOC and S_N numerical methods. Even though these two methods are totally different, it is worth noting that total number of cases that acheive a given precision ϵ is quite similar. This can be explicited by realising that this suite of problems is defined by a large variation in space parameters, generating approximately the same number of pathologic cases for MOC and S_N methods. We also display in Figures 7 to 12 the mean relative error by case for the three values of L.

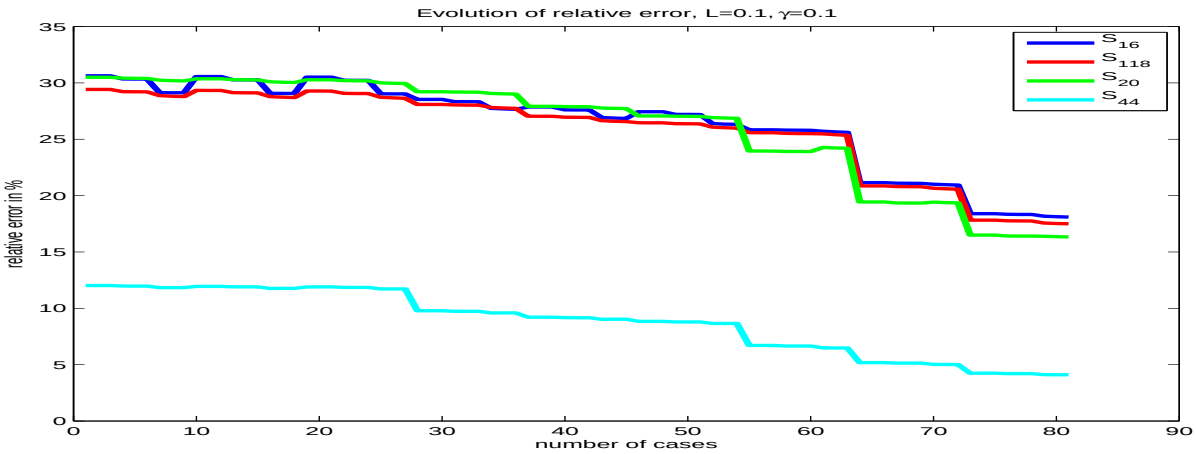

Figure 7: S_N results for $L = 0.1$.

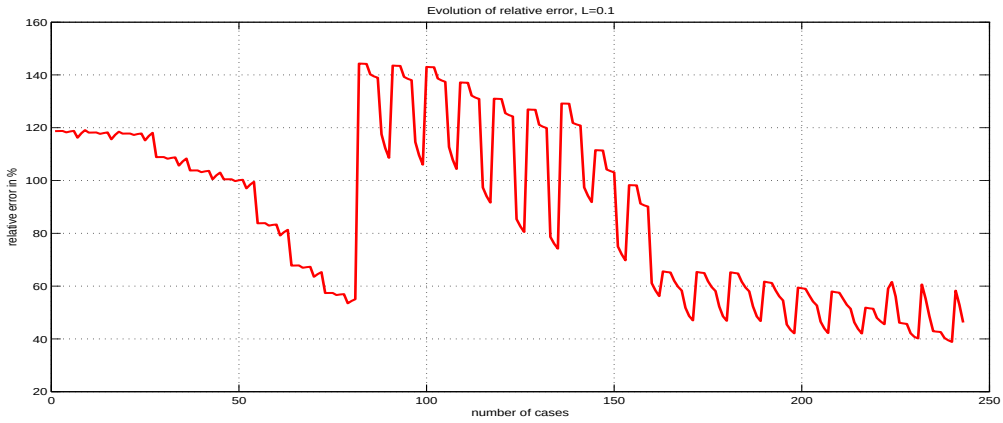

Figure 8: MOC results for $L = 0.1$.

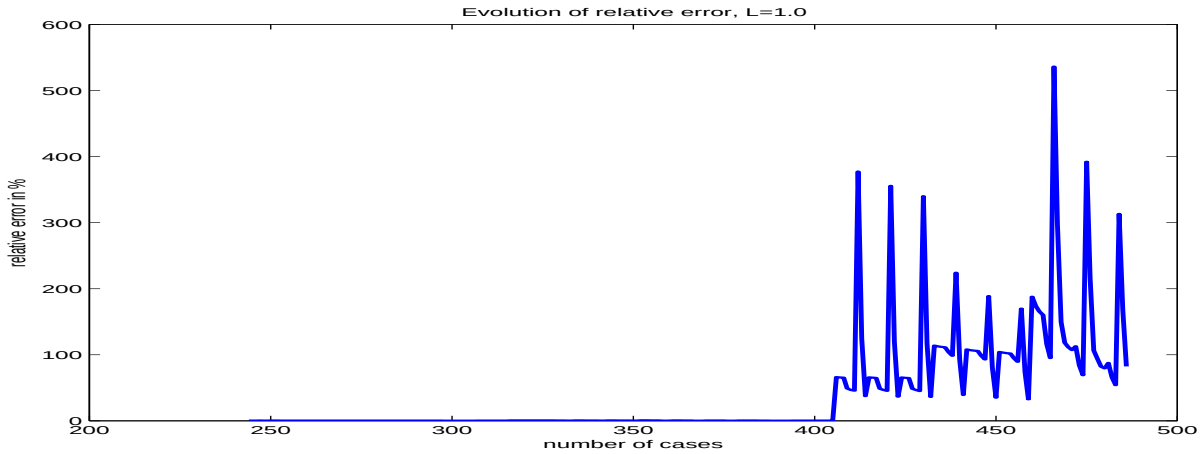

Figure 9: S_N results for $L = 1.0$.

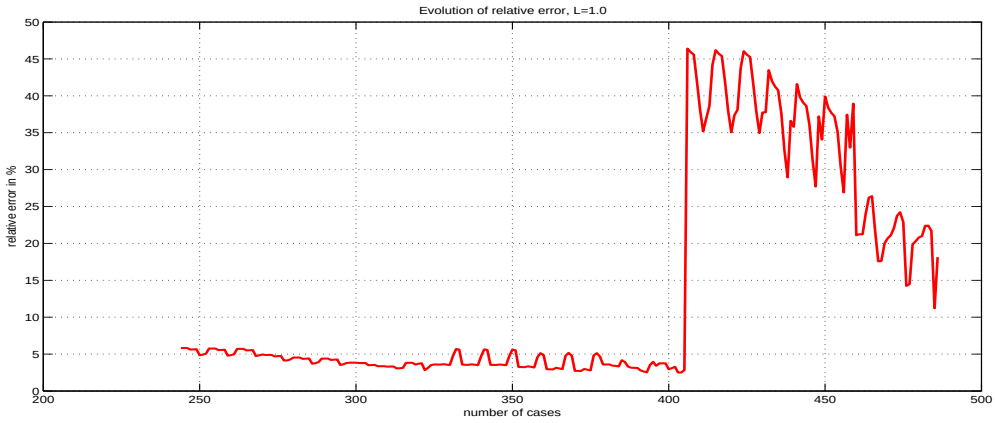

Figure 10: MOC results for $L = 1.0$.

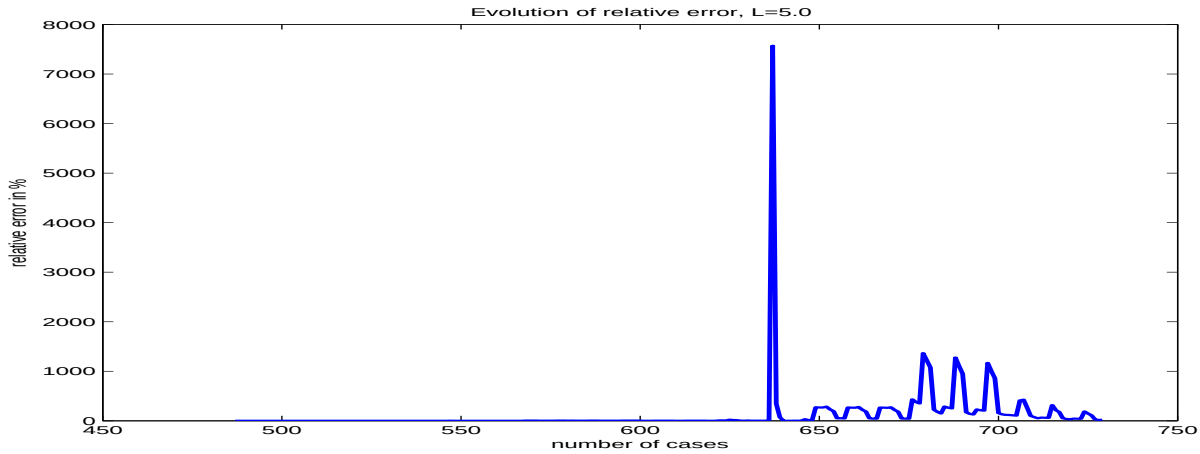

Figure 11: S_N results for $L = 5.0$.

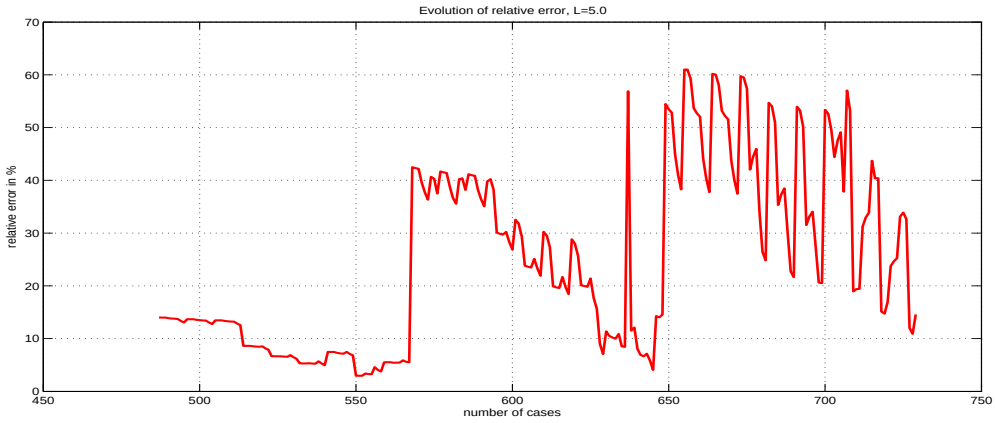

Figure 12: MOC results for $L = 5.0$.

Concentrating first on the S_N relative error, one observes that strong peaks appear for cases in which $\Sigma_1 = \Sigma_2 = 5.0$. Peaks are getting wose when L=5.0, due to the combined fact that source dimension is reduced and attenuation is high. Another class of problematic cases are when $\Sigma_i = 0.1$ and $\Sigma_j = 5.0$. This define a strong heterogeneous media combined with a highly localized neutron source. As a result, ray effects start to dominate the errors in the S_N method and the computed fluxes oscillate seriously and become non physical.

MOC solutions suffer globally in the same configurations especially in high absorbing/diffusive or heterogeneous cases ($\Sigma_1 = \Sigma_2 = 5.0$ or $\Sigma_i = 50 \times \Sigma_j$), altough the dimensions of the source play an key role in the precision of the solution. As γ is growing, the source dimension is reduced, and the MOC computed error exceeds by far the S_N errors. This is mainly a consequence of the flat source approximation, which is non valid in some configurations.

VIII. Conclusion

The NEA3D-TAB-2007 benchmark study was intended to observe limitations of deterministic methods, and to help reactor physicists propose new improvements for this class of numerical methods. We first conclude that for the MCNP reference solutions with acceptable statistical errors, both S_N and MOC methods reach a level of accuracy close to the Monte-Carlo results. Moreover, other deterministic solutions such as produced by the IDT code [11] have similar relative errors. However, DRAGON-S_N results suffer deeply in some configurations ($L = 5.0$) from ray effects, a typical shortcoming appearing in case of strong heterogeneous medias. Rising the quadrature order has been established as the most powerfull solution to avoid this restriction. As a consequence, new angular quadratures have been implemented, such as QR (quadruple Range) quadrature up to the S_{72} order [12]. For the MOC method, if bad angular discretization is also an important issue, an inadequate spatial mesh discretization detoriorates the flat source approximation and leads to a rapid growth of the numerical errors. Finally, an important issue is also computational time. In this case, the S_N method was far more advantagous than the MOC method. To complete this study, it would be interesting to compare CPU time for S_N and MOC methods with that of MCNP.

REFERENCES

[1] G. Marleau, A. Hébert, R. Roy, "A User Guide for DRAGON Version4", *Report IGE-294*, Institut de Génie Nucléaire, Ecole Polytechnique de Montréal, (2007).

[2] R. Le Tellier, "Développement de la méthode des caractéristiques pour le calcul de réseau", *PhD thesis*, Institut de Génie Nucléaire, Ecole Polytechnique de Montréal (2006).

[3] N. Martin, A. Hébert, "Application of high-order diamond differencing to 3D Cartesian Geometries", *PHYSOR-2008, Int. Conf. on the physics of reactors*, September 14-19, Interlaken, Switzerland, (2008).

[4] NEA/NSC Expert group on 3D radiations transport benchmarks, *Benchmarking the Accuracy of Solution of 3-Dimensional Transport Codes and Methods over a Range in Parameter Space, NEA/NSC Documentation*, (2007).

[5] R. Le Tellier, A. Hébert, "An improved algebraic collapsing acceleration with general boundary conditions for the characteristics method", *Nuclear Science and Engineering*,**156**, 121-138 (2007).

[6] G. J. Wu, R. Roy, "Self-collision rebalancing technique for the MCI characteristics solver". *In Proc. of the 20th Annual Conf. of the Canadian Nuclear Society, Montréal, CNS*, (1999).

[7] K. B. Bekar, Y. Y. Azmy, "TORT Solutions to the NEA Suite of Benchmarks for 3D Transport Methods and Codes over a Range in Parameter Spaces", *PHYSOR-2008, Int. Conf. on the physics of reactors*, September 14-19, Interlaken, Switzerland, (2008).

[8] M. L. Adams, E. W. Larsen, "Fast Iterative Methods for Discrete Ordinates Particles Transport Calculations", *Progress in Nuclear Energy*, **40**, 3-159 (2002).

[9] R. E. Alcouffe, Diffusion Synthetic Acceleration Methods for the Diamond-Differenced Discrete-Ordinates Equations, *Nuclear Science and Engineering*, **64**, 344-355 (1977).

[10] Y. Saad, M. H. Schultz, GMRES : A Generalized Minimal RESidual Algorithm For Solving Nonsymmetric Linear Systems, *SIAM Journal on Scientific and Statistical Computing*, **7**, 856-869 (1986).

[11] I. Zmijarevic, "IDT solution to the 3D transport benchmark over a range in parameter space", *PHYSOR-2008, Int. Conf. on the physics of reactors*, September 14-19, Interlaken, Switzerland, (2008).

[12] I. K. Abu-Shumays, "Angular quadratures for improved transport computations", *Transport Theory and Statistical Physics*, **33**, 169-204 (2001).